Why the hadronic gas description of hadronic reactions works: the example of strange hadrons

P. Koch and J. Rafelski
Institute of Theoretical Physics and Astrophysics, University of Cape Town, Rondebosch

The degree to which, in hadronic reactions, the strangeness quark flavour is equilibrated in its abundance with the light quarks' flavours is proposed as a measure of the relevance of gluonic degrees of freedom in hadronic reactions. The transitory presence of gluons manifests itself by generating strange quark abundance near the hadronic gas equilibrium in pp and pN reactions. Nucleus–nucleus collisions below 5 GeV/n appear to be in the regime of individual nucleon collisions in which the intrinsic QCD degrees of freedom are frozen. In consequence, the measured strangeness abundance in these nuclear collisions falls short of the values expected from the hadronic gas equilibrium. Should the quark–gluon plasma state be formed at higher energies, the signal for this process would be the equilibration of total strangeness abundance almost as if an equilibrated hadronic gas had been formed. Anomalies in the abundance of strange antibaryons remain the characteristic and global signal of plasma state formation.

S. Afr. J. Phys. 9 (1986) 8–23

Die mate waartoe die konsentrasie van vreemde kwarke by hadroniese reaksies in ewewig met die konsentrasie van ligte kwarke kom, word voorgestel as 'n maatstaf van die belangrikheid van gluonvryheidsgrade. Die verbygaande teenwoordigheid van gluone self kom tot uitdrukking deur vreemde kwarke naby die hadrongasewewig in pp- en pN-reaksies voort te bring. Kern–kern-botsings onderkant 5 GeV/n is skynbaar in die gebied van individuele nukleonbotsings waarin die intrinsieke QCD-vryheidsgrade 'gevries' bly. Die gemete vreemdheidkonsentrasie in hierdie kernbotsings is dus laer as die waardes wat uit die hadrongas-ewewig verwag word. Indien die kwark–gluon-plasma by hoër energiewaardes gevorm sou word, sou die teken hiervoor die ekwilibrasie van die totale konsentrasie van vreemdheid wees, byna asof 'n hadrongas in ewewig ontstaan het. Anomalieë in die konsentrasie van vreemde antibarione bly die kenmerk en globale sein van die totstandkoming van 'n plasmatoestand.

S.-Afr. Tydskr. Fis. 9 (1986) 8–23

P. Koch* and J. Rafelski
Institute of Theoretical Physics and Astrophysics,
University of Cape Town,
Rondebosch 7700, Republic of South Africa
*Visitor from the Institut für Theoretische Physik
der Johann Wolfgang Goethe Universität, Frankfurt am Main,
Federal Republic of Germany

Received 28 August 1985

1. Introduction

The observation that soft multihadron production ($p_\perp <$ 1 GeV) shows many features of an underlying statistical reaction mechanism has inspired Hagedorn's Statistical Bootstrap [1, 2] long before anything about quantum chromodynamics (QCD) was known. But since QCD has been accepted as the underlying gauge field theory of strong interactions, it seems today rather 'oldfashioned' to treat high energetic hadronic collisions in the framework of phenomenological statistical models. A contrary understanding may be adopted following the present discussion. Our point of view is that the transitory formation of a quark–gluon plasma-like state is the prerequisite in order that statistical models can be used. The number of accessible states in hadronic reactions may be many times larger than a naive hadronic phase space counting indicates and a statistical description may indeed also be necessary in order to describe the hadronic interactions. The whole hadronic reaction system does not need to participate in the statistical part of the reaction. For example, in high energetic central p–p collisions the valence quarks penetrate the reaction region without much interaction, while the energy and momentum in the gluon field dominates the central rapidity reaction region by virtue of the much larger statistical weight of gluons [3]. In this and other similar approaches it is assumed that a domain in space arises in a centre-of-momentum frame in which an important part of the longitudinal energy is transferred to transverse degrees of freedom. Such regions of space we call 'fireball'. The physical variables characterizing the fireball domain are energy density, baryon number density, and volume. When considering high-energy hadronic interactions, we mostly investigate the internal structure and the time evolution of this fireball, except for the rare high $p_\perp$ phenomena which arise due to the hard scattering processes.

The most immediate question which arises here concerns the internal structure of the fireball:

(i) Does it consist of individual hadrons with short-range correlations between the constituent quarks? Is the reaction therefore governed by interactions between individual hadronic resonances?

(ii) Or, does it consist of the quark–gluon plasma phase where short-range colour correlations are broken [4] and in which quarks and gluons are the active constituents?

The experime

two types of fireballs, viz. the distinction of the quark–gluon plasma from the hadronic gas, is facilitated by the presence of numerous gluons only in the plasma phase. Depending on which statement is more appropriate in a particular collision process, strong influence on the equilibration properties of these two realizations of hadronic matter is encountered. In case (i) of hot hadronic gas, the gluonic degrees of freedom remain frozen and confined to the volumes of the individual hadrons. In case (ii), in the quark–gluon plasma region of space, gluons are excited and participate in the overall process of equilibration. But since gluons carry colour, the charge of strong interactions, their detection in an experiment can only be indirect, as colour is confined. But gluons turn out to be very efficient in generating strange-quark pairs in quark–gluon plasma [5] and hence transitory presence of gluons may be inferred from the appearance of high strangeness abundance. In order to appreciate this remark, one first has to recognize that the basic subprocess for strange-quark production, namely the pair production process $gg \rightarrow s\bar{s}$, is, in principle, the same for both phases of hadronic matter. In the case of well-separated hadrons with the true non-perturbative QCD vacuum inbetween, the above-mentioned reaction can only take place during the actual collision process of two individual hadrons, which means that strange-quark production experiences severe constraints in space and time. Furthermore, all initial- and final-state hadrons are colour singlets and the effective number of the available degrees of freedom is greatly reduced in comparison to the quark–gluon phase. The actual degree of colour-freezing is dependent on the volume and intrinsic temperature of hadronic gas constituents [6, 7] but is effective as long as individual hadrons remain undissolved. These arguments provide the basis for the proposal [8] that abundances of certain strange hadrons provide a characteristic signal about the gluon abundance.

In this work we will compare the present experimental data on strange-particle production with theoretical calculations of the approach to equilibrium saturation of strange-particle abundances in both phases of the hadronic world. We conclude that the state of the qualitative chemical equilibration between light and strange flavours, as observed in high energetic hadronic collisions, could only be achieved if a transitionary state similar in its main characteristics to the thermally excited quark–gluon matter has been formed in the early stages of the collision process. In the particular case of nucleus–nucleus collisions the available experimental data show that nuclear collisions at 1.8 GeV/A kinetic energy [9] are dominated by collisions between individual hadrons, indicating that the threshold for quark–gluon matter is not exceeded at this collision energy. We expect to produce a quark–gluon plasma state over a larger domain in space and time as we apparently can do in hadron–hadron or hadron–nucleus collisions when the kinetic energy is too small.

We commence in the next section with the description of the quark–gluon phase and in particular, equilibrium abundance and strange quark formation reactions. In section 3 similar considerations are presented concerning the hadronic gas phase and a pre-equilibrium comparison of effects arising from both phases is made. In section 4 comparison with the experiment leads us to the conclusions spelled out in the above paragraphs.

2. Strangeness in quark–gluon plasma

2.1 $\bar{q}$ and $\bar{s}$ saturated phase space in quark–gluon plasma

One of the reasons why strange-particle abundance is characteristic for the formation of the quark–gluon plasma is, as we first calculate, the anomalously high abundance of strange quarks we expect if the whole phase space provided for by the quark–gluon plasma system were saturated.

Recall that at a given temperature the quark–gluon plasma will contain an equal number of strange quarks, s, and antistrange quarks, $\bar{s}$ [8], as strangeness can only be created or annihilated in pairs, disregarding here the slow weak interaction processes. Thus in a chemical and thermal equilibrated quark–gluon plasma, we find for the density of strange and antistrange quarks (neglecting QCD perturbative corrections):

$$\frac{s}{V} = \frac{\bar{s}}{V} = g_s \int \frac{d^3P}{(2\pi)^3} \frac{1}{(e^{\sqrt{P^2+m_s^2}/T}+1)} \tag{2.1a}$$

where $g_s = 6$ for spin and three colour degrees of freedom and m_s is the strange-quark mass, that is, the effective mass parameter of the basic reaction processes. In the case of a high-temperature quark–gluon plasma, we expect to be in the regime where the quark masses are represented by their current masses. Recent studies [10] place the running strange-quark mass at $m_s \approx 180$ MeV at $Q \approx 1/2 - 1$ GeV. Thus m_s appears to be of the same magnitude as the critical temperature T_c for the phase transition to quark–gluon plasma, $T_c \approx 180$ MeV [7]. We find after expanding eq. (2.1a),

$$\frac{s}{V} = \frac{\bar{s}}{V} = \frac{3T^3}{\pi^2}\left(\frac{m_s}{T}\right)^2 \sum_{n=1}^{\infty} \frac{(-)^{n-1}}{n} K_2\left(\frac{nm_s}{T}\right), \tag{2.1b}$$

where $K_2(x)$ is as usual the modified Bessel function.

For the light-antiquark density ($\bar{q}$ stands for either $\bar{u}$ or $\bar{d}$) we can write

$$\frac{\bar{q}}{V} = 6 \int \frac{d^3P}{(2\pi)^3} \frac{1}{(e^{|P|/T+\mu_q/T}+1)} \tag{2.2}$$

where we have introduced a chemical potential of light quarks, μ_q. Since each baryon contains three quarks we further have a relation to the chemical potential of baryons:

$$\mu_B = 3\mu_q. \tag{2.3}$$

Finite baryon density corresponds to finite μ_q and reduces the required critical temperature for formation of the plasma state [11]. As one can see from eq. (2.2), the chemical potential of the quarks suppresses the $\bar{q}$ density. This phenomenon reflects on the chemical equilibrium between $q-\bar{q}$ and the presence of a light-quark density associated with the net baryon number B. (The $\bar{q}$ are easily destroyed by the abundant q's when the q density is large, hence their reduced abundance.)

It is possible to expand the integral (2.2) in a manner analogous to eq. (2.1b) and we obtain the following ratio ($\mu_q > 0$):

$$\frac{\langle \bar{s} \rangle}{\langle \bar{q} \rangle} = \frac{1}{2} \frac{\sum_{n=1}^{\infty} \frac{(-)^{n-1}}{n^3} \left(\frac{nm_s}{T}\right)^2 K_2\left(\frac{m_s n}{T}\right)}{\sum_{n=1}^{\infty} \frac{(-)^{n-1}}{n^3} e^{-n\mu_q/T}} \tag{2.4}$$

which is depicted in Figure 2.1. Here $\bar{q}$ includes both the $\bar{u}$ as well as the $\bar{d}$ quarks. The strong suppression of $\bar{q}$ in the limit of large μ_q, that is in cases of substantial baryon densities, is clearly visible. Interesting enough one finds even in the limit of a $q-\bar{q}$ symmetric system, i.e. baryon number $B = 0$, a similar number of $\bar{s}$ quarks as there are $\bar{u}$ or $\bar{d}$ quarks as long as $T \approx m_s$. This remark will be of interest as it suggests that the strange quarks can compete in abundance with the 'ordinary' antiquarks even at moderate temperatures.

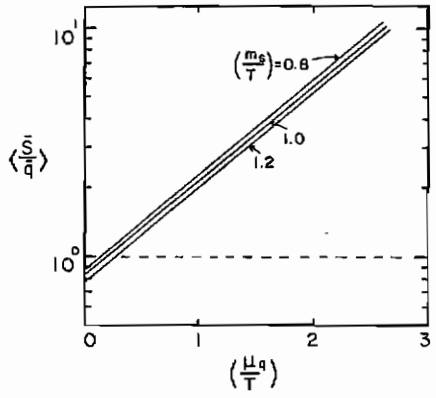

Figure 2.1 Abundance ratio for $\bar{s}/\bar{q}$ quarks as a function of chemical potential μ measured in units of T, for several choices of $m_s/T = 0.8$, 1.0 and 1.2.

2.2 Approach to the saturated phase space limit

One may wonder about the validity of assuming thermal and chemical equilibration in a state of matter existing during the short period of a high energetic collision process between nuclei. Hence, we now discuss the approach to the chemical equilibrium of s-quarks, initially in the quark–gluon plasma phase.

In lowest order in perturbative QCD, $s\bar{s}$ quark pairs can be created by annihilation of light quark–antiquark pairs (Figure 2.2b) and in collisions of two gluons (Figure 2.2a). The averaged total cross-sections for these processes were calculated by Combridge [12a]. For a fixed invariant mass-squared $s = (k_1 + k_2)^2$ (note that this s is not related to the strangeness 's') where k_i are the four momenta of the incoming particles, we have

$$\bar{\sigma}_{q\bar{q}\to s\bar{s}} = \frac{8\pi\alpha_s^2}{27s}\left(1 + \frac{2M^2}{s}\right) W(s) \tag{2.5}$$

$$\bar{\sigma}_{gg\to s\bar{s}} = \frac{2\pi\alpha_s^2}{3s}\left\{\left[1 + \frac{4M^2}{s} + \frac{M^4}{s^2}\right]\tanh^{-1} W(s) - \left[\frac{7}{8} + \frac{31}{8}\left(\frac{M^2}{s}\right)\right] W(s)\right\} \tag{2.6}$$

with

$$W(s) := \left(1 - \frac{4M^2}{s}\right)^{1/2}. \tag{2.7}$$

Given the averaged cross-sections it is easy to calculate the rate of events per unit time summed over all final and initial states:

$$\frac{dN}{dt} = \int d^3x \int \frac{d^3k_1}{(2\pi)^3} \sum_i \rho_i(k_1, x) \int \frac{d^3k_2}{(2\pi)^3} \times \tfrac{1}{2} \sum_i \rho_2(k_2, x) \int_{4m_s^2}^{\infty} ds\, \delta[s - (k_1 + k_2)^2] \bar{\sigma}(s). \tag{2.8}$$

The sum over the initial states involves the discrete quantum numbers i (colour, spin, etc.) over which eqs. (2.5) and (2.6) were averaged. The factor $\frac{1}{2}$ avoids double counting of particle pairs. In order to facilitate the calculations, a dummy integration over s was introduced.

To proceed further, we have to specify phase space densities denoted here by $\rho_i(k_i x)$. Perturbative QCD calculations show that due to the colour degrees of freedom the $gg \to gg$ process first order in α_s has a large cross-section [12b] indicating a rather short mean free path for gluons. Furthermore, the anticipated lifetime of the plasma created in a nuclear collision is about 6 fm/c = 2×10^{-23} s, and it may be formed at an energy density of approximately 1 GeV/fm^3. Under these conditions of ca 2 particles/fm^3, it seems that each quark or gluon will rescatter several times during the lifetime of the plasma. One should recall here that randomization of the particle momenta leading to a Boltzmannian distribution requires only very few collisions. Thus we can approximate the momentum distribution functions in eq. (2.8) by the quantum statistical distribution functions, i.e.

$$\rho_i(k_i, x) \to f(k_i) \tag{2.9}$$

where

$$f_g(k) \approx (e^{\beta k} - 1)^{-1} \quad \text{(gluons)} \tag{2.10a}$$

$$f_{\bar{q},q}(k) \approx (e^{\beta k \pm \beta\mu_q} + 1)^{-1} \quad \text{(anti, -quarks)} \tag{2.10b}$$

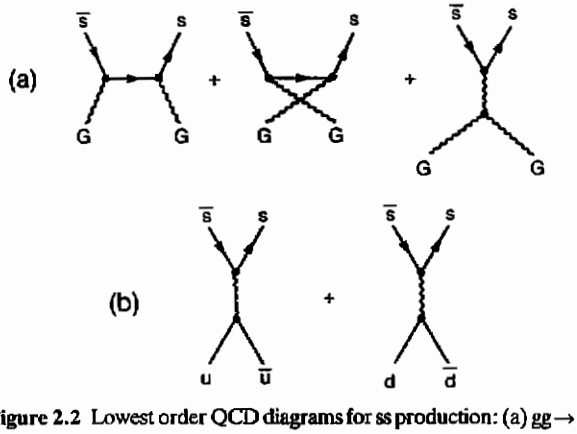

Figure 2.2 Lowest order QCD diagrams for ss production: (a) $gg \to s\bar{s}$; (b) $q\bar{q} \to s\bar{s}$.

where $\beta\mu$ is the covariant temperature, $\beta k = \beta_0|\vec{k}| - \vec{\beta}\cdot\vec{k}$ for massless particles, $(\beta\beta)^{-1/2} = T$ is the temperature in the rest frame.

With $n_s(\infty)$ being the saturation density at large times, the following differential equation governs the time evolution of n_s;

$$\frac{dn_s}{dt} \approx A\left\{1 - \left[\frac{n_s(t)}{n_s(\infty)}\right]^2\right\}, \tag{2.11}$$

where

$$A = \frac{dN}{dt\, d^3x} \tag{2.12}$$

is the rate per unit time and unit volume obtained from eq. (2.8). We note that eq. (2.11) may also include a term linear in $n_s(t)$, namely, when the plasma density is sufficiently high the produced strange quarks have difficulty in getting away quickly from each other. With a scattering length of the order of 1/3 fm, in extreme cases, one has to allow for diffusion rather than ready free motion. In the limiting case of very dense medium we find an $s\bar{s}$ pair in a given correlation volume, and hence the annihilation term is linear in n_s:

$$\frac{dn_s}{dt} \approx A\left\{1 - \left[\frac{n_s(t)}{n_s(\infty)}\right]\right\}. \tag{2.13}$$

The solutions of eqs. (2.11) and (2.13) are quite similar in their appearance and are, respectively,

$$n_s(t) = n_s(\infty)\tanh(t/2\tau) \xrightarrow[t\to\infty]{} n_s(\infty)(1 - 2e^{-t/\tau}) \tag{2.14}$$

$$n_s(t) = n_s(\infty)[1 - e^{-t/2\tau}] \tag{2.15}$$

with the relaxation time constant

$$\tau = n_s(\infty)/2A.$$

After suitable approximations [5], we obtain

$$\tau \approx \tau_g \simeq \frac{1.61}{\alpha_s^2 T} \frac{\left(\frac{m_s}{T}\right)^{1/2} e^{m_s/T}}{\left(1 + \frac{99}{56}\frac{T}{m_s} + \ldots\right)}, \tag{2.16}$$

where the inferior index g denotes the dominant gluon contribution to the $s\bar{s}$ pair production process.

Using the fact that the ratio of (m_s/T) will be, in general, approximately equal to one we can write for eq. (2.16),

$$\tau_g \simeq \frac{1}{\alpha_s^2 m_s} \tag{2.17}$$

which gives an approximate value of $\tau_g \simeq 1 \times 10^{-23}$ s if $\alpha_s \simeq 0.6$ and $m_s \simeq 150$ MeV. We hence record that the strangeness abundance will have time to achieve near chemical saturation for lifetimes of a quark–gluon plasma state of the order of 2×10^{-23} s. This circumstance is illustrated quantitatively in Figure 2.3 where the evolution of strange-quark to baryon abundance is shown as function of time with T being the parameter.

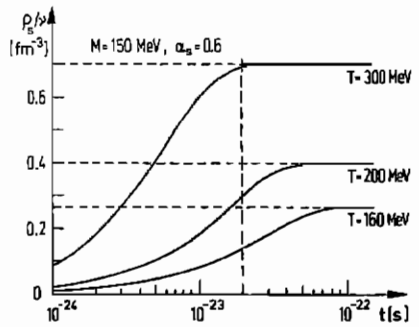

Figure 2.3 Time evolution of the relative strange-quark to baryon number abundance in the plasma for various temperatures T (m_s = 150 MeV, α_s = 0.6).

We mention at this point that the process of formation of charmed quarks in a quark–gluon plasma is quite different due to the fact that $(m_{charm}/T) \approx 10$ and we have, provided that high-energy gluons are available for such a far-off-thermal equilibrium reaction,

$$\tau_g^{charm} \to \frac{10^5}{\alpha_s^2 m_{charm}} \approx 1 \times 10^{-19}\,\text{s}. \tag{2.18}$$

This result implies a very low charmed-quark abundance at the break-up time of the quark–gluon plasma which is expected to live not much longer than 2×10^{-23} s, and we also note here the absence of hard gluons in the plasma.

So it turns out that it is just the small window — quark mass equal to temperature — which allows us to observe the presence of a quark–gluon plasma by the large abundance of strangeness created by gluons during the short lifetime of the plasma state.

2.3 Discussion

We thus conclude that the strangeness abundance saturates in a sufficiently excited quark–gluon plasma with $T >$ 160 MeV, $\varepsilon > 1$ GeV/fm^3, owing to the high gluon density. This allows strangeness to be an important observable indicating the abundant presence of gluons in the reaction.

When the quark matter hadronizes, some of the numerous s and $\bar{s}$ quarks may form strangeness clusters such as Ξ, Ω, and their antiparticles, and also exotic strange objects, instead of being bound in kaons only. If the plasma state froze out directly into a low-density hadron gas, we would end up, as can easily be argued (see section 3.3), with a very large abundance of strange hyperons and antihyperons. These abundances would give us the upper limit we can expect from the quark–gluon plasma. In a real collision process, this high hyperon abundance will be depleted by the processes of expansion and mixing with the remainder of non-participating hadronic gas matter. The QGP over-abundance may therefore be reduced down to the equilibrium abundances as given by the hadronic gas phase but would, at that level, still be very much larger than otherwise expected.

In order to appreciate the strange-particle abundances emerging from QGP, we have to study, in detail, the case where no QGP has formed and hadronic matter consists of individual hadrons. In particular, the approach to chemical equilibrium abundances will be of greatest importance and it will turn out that it is the absence of the equilibrium abundances in the hadronic gas phase which distinguishes

between the two different states of hadronic matter. Thus QGP acts like a source of strangeness, facilitating rapid saturation of the (hadronic gas) phase space. Absence of gluonic degrees of freedom assures that far too little strangeness is produced in individual hadronic (gas) collisions.

3. Strangeness in hadronic gas

In order to gain a deeper insight into the relevance of strangeness as a characteristic signature of the quark–gluon plasma, we now turn to the study of strangeness in the hadronic gas (HG) phase. As we have done in the case of the QGP we will first consider the phase space saturated state of the HG. In principle, the HG is a very complicated object due to the presence of numerous hadronic resonances. But it turns out that just the postulate of the resonance-dominance of hadron–hadron interactions [1c, d], allows us to simplify the calculation. In this case the hadronic gas phase is a superposition of different hadronic gases and all information about the interaction is hidden in the mass spectrum $\tau(m^2,b)$ which describes the number of hadrons of baryon number B in a mass interval dm^2. When considering strangeness-carrying particles, all we then need is to include the influence of the non-strange hadrons as providing the chemical potentials, corresponding to quantum numbers like baryon number or electric charge of the non-strange particles. The total partition function is nearly additive in these degrees of freedom:

$$\ln Z = \ln Z^{\text{non-strange}} + \ln Z^{\text{strange}}. \tag{3.1}$$

In order to determine strange-particle abundances at fixed μ_B, it is sufficient to study $\ln Z^{\text{strange}}$ only.

3.1 Strange-particle abundances from HG in chemical equilibrium

Consider

$$\ln Z^{\text{strange}}(V,T,\lambda_i) = \sum_j Z_j \prod_{i=B,s,Q,\ldots} (\lambda_i^{(j)})^{n_{ji}} \tag{3.2}$$

where the one-particle Boltzmann partition functions

$$Z_j = Z_j(V,T) = g_j\left(\frac{VT^3}{2\pi^2}\right)\left(\frac{m_j}{T}\right)^2 K_2\left(\frac{m_j}{T}\right) \tag{3.3}$$

of the particle species j with the corresponding degeneracy factor g and mass m appear. Because of the low density of strange particles in hadronic matter, the use of Boltzmann statistics is justified. The fugacities λ_i as introduced in eq. (3.2) control the quantum number content of the species j. We will, in particular, use λ_s which controls the strange-quark content, λ_B which controls the baryon number content and later on also a λ_Q associated with the electric charge. The power n_{ji} is the number of charges 'i' in the hadron 'j'.

Using the partition function (3.2), we can calculate the mean strangeness by evaluating

$$\langle n_s - n_{\bar{s}} \rangle = \lambda_s \frac{\partial}{\partial \lambda_s} \ln Z^{\text{strange}}(V,T,\lambda_s,\ldots) \tag{3.4}$$

which is the difference between strange and anti-strange components. This expression must be equal to zero since strangeness is a conserved quantum number with respect to the strong interactions. This introduces an important constraint, e.g. it fixes λ_s in terms of λ_B (for $\lambda_Q = 1$). Let us ignore, in the first instance, the multistrange particles Ξ and Ω^- as well as λ_Q and consider only kaons, Λ's and Σ's. Then we get from eq. (3.4),

$$\lambda_s' = \left[\frac{Z_K + \lambda_B^{-1} Z_Y}{Z_K + \lambda_B Z_Y}\right]^{1/2}, \tag{3.5}$$

where

$$Z_Y = Z_\Lambda + Z_\Sigma. \tag{3.6}$$

What we notice is a strong dependence of λ_s on the baryon number. Since, as usual,

$$\lambda_B = e^{\mu_B/T}, \tag{3.7}$$

the term with λ_B^{-1} will tend to zero as μ_B gets large and the term with λ_B will dominate the expression for λ_s'. As a consequence the particles with fugacity λ_s' and strangeness $s = -1$ (note that by convention, strange quarks carry $s = -1$, while strange antiquarks carry $s = 1$) are suppressed by λ_s which is always smaller than unity. Conversely, the production of particles which carry the strangeness $s = +1$ will be favoured by $\lambda_s'^{-1}$. This is due to the presence of finite nuclear matter density. Only $q\bar{s}$ kaons are permitted as carriers of $\bar{s}$ quarks. In other words, $q\bar{s}$ states (K^+) are carriers of $\bar{s}$ quarks, while qqs states (hyperons) are main carriers of s quarks at finite baryon density.

In order to calculate mean abundance of strange particles, we introduce for each species its own dummy fugacity (which we subsequently will set equal to unity) and proceed under the assumption that the different strange particles are in mutual chemical equilibrium. Whether this assumption is justified will be of concern in the next section where we proceed to study the detailed time evolution of strange hadrons and the here relevant strangeness exchange reactions. We may expect that certain rare strange hadrons will not satisfy this assumption while kaons and hyperons might.

The strange-particle multiplicities are obtained from

$$\langle n_j \rangle = \lambda_j \frac{\partial}{\partial \lambda_j} \ln Z_0^{\text{strange}}\Big|_{\lambda_i=1} \tag{3.8}$$

where Z_0^{strange} denotes the grand canonical partition sum for zero average strangeness.

In Figures 3.1a, 3.1b and 3.1c we show three examples, namely, the ratios of antihyperons to hyperons. The explicit expressions for these ratios turn out to be very simple:

$$\frac{\langle n_{\bar{\Lambda}} \rangle}{\langle n_\Lambda \rangle} = \lambda_B^{-2}\lambda_s^{-2} \tag{3.9a}$$

$$\frac{\langle n_{\bar{\Xi}} \rangle}{\langle n_\Xi \rangle} = \lambda_B^{-2}\lambda_s^{-4} \tag{3.9b}$$

$$\frac{\langle n_{\bar{\Omega}} \rangle}{\langle n_\Omega \rangle} = \lambda_B^{-2}\lambda_s^{-6} \tag{3.9c}$$

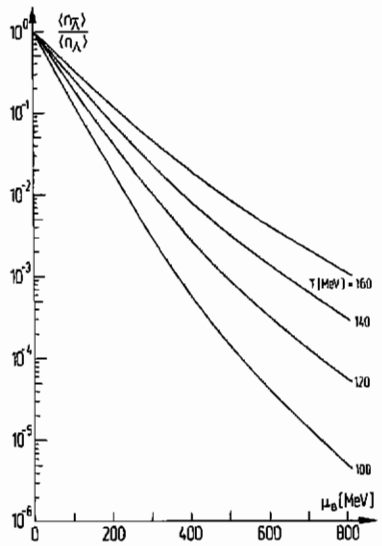

Figure 3.1a Ratio of $\bar{\Lambda}/\Lambda$ in dependence on baryochemical potential μ_B at fixed temperatures T. Hadronic gas equilibrium.

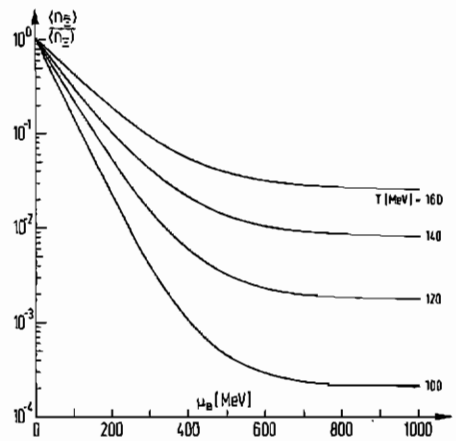

Figure 3.1b Ratio of $\bar{\Xi}/\Xi$ in dependence on the baryochemical potential μ_B at fixed temperatures T. Hadronic gas equilibrium.

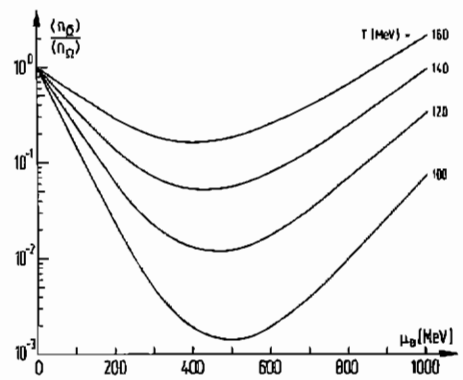

Figure 3.1c Ratio of $\bar{\Omega}/\Omega$ in dependence on the baryochemical potential μ_B at fixed temperatures T. Hadronic gas equilibrium.

λ_s is slightly different [13] from λ_s' as defined in eq. (3.5), since we have further included in eq. (3.2) multiple strange baryons. Through the enhancement of antistrangeness due to λ_s^{-1} the ratio $\bar{\Omega}/\Omega$ (Figure 3.1c) loses the memory of the baryon number content and approaches for large temperatures unity over the whole μ_B region. We expected such a behaviour only if these particles are produced from a QGP and we will show below that dynamics of the reactions restores the validity of the intuitive argument that quark–gluon plasma facilitates formation of multiple strange hadrons. The appearance of enhanced Ω abundance in equilibrium hadronic gas calculations is a consequence of the unwarranted assumptions about the relaxation time constants of these rare states, as will be discussed in section 3.2 below. The abundance of $\bar{\Omega}$ can be significant only if QGP has been formed.

In Figure 3.1a the expected suppression of $\bar{\Lambda}$ due to the baryo-chemical potential as well as the strangeness chemistry is recorded. This ratio exhibits both a strong temperature- and μ_B-dependence. The remarkably small abundance of $\bar{\Lambda}$, e.g. $10^{-4}\Lambda$ in hadronic gas phase, under conditions likely to be reached in an experiment at the end of the hadronization phase [$T \approx 120-180$ MeV, $\mu_B \approx (4-6)T$] is characteristic of the nuclear nature of this hot hadronic matter phase. Naive estimates for the quark–gluon plasma $\bar{\Lambda}/\Lambda$ abundance based on flavour content, are two to three orders of magnitude higher. The actual abundance of antihyperons in the hadronic gas or quark–gluon plasma phases must be computed in an off-equilibrium approach and the here presented equilibrium ratios are to be taken as upper limits in the instance that no quark–gluon plasma has been formed.

We further note that even assuming absolute chemical equilibrium in the gas phase, we still find 3 to 5 times more strangeness in the plasma at comparable thermodynamic parameters, i.e. equal μ, T. This is shown in Figure 3.2 as a function of μ_B at some selected values of T and m_s, where the conversion from μ_B as a variable to baryon density has been done using perturbative QCD expression.

The corresponding baryon density in the hadronic phase is much lower if a first-order phase transition is encountered. Due to this effect, the total equilibrium strangeness abundance is nearly equal in both hadronic phases, as

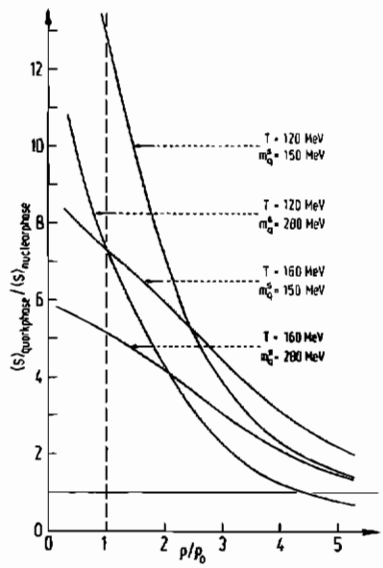

Figure 3.2 Ratio of strangeness along the transition line between the plasma and the hadronic gas phase as a function of assumed baryon density on the plasma side.

pointed out by Redlich [14]. However, the approach to equilibrium would be even further delayed in the thinner gas phase. Thus all strangeness is always produced in QGP phase simply because the density of gluons is so extraordinarily enhanced there, owing to their colour degeneracy factor 8 and their masslessness.

3.2 Approach to chemical equilibrium abundances in hadronic gas

Until here in our calculations for the hadronic gas phase we were assuming that all strange particles, firstly, are in mutual chemical equilibrium among themselves, and secondly, that the available phase space is saturated. The first assumption arises from the observation that through relatively large strangeness exchange cross-sections [15], strangeness (once produced) is readily redistributed very fast over the whole strange-particle family.

We intend now to quantify our knowledge about the dynamics of both strangeness production and redistribution in the hadronic gas phase and proceed to compute the time scales involved in strangeness production and exchange reactions, with particular emphasis put on the case of multiple-strangeness-carrying antibaryons. In doing so, we extend our chemical equilibrium model to the pre-equilibrium conditions and set up a set of evolution equations for the strange-particle family in the spirit of chemical reaction (kinetic) equations. Such an approach has previously been considered by Mekjian [16], but not so for the case of multiply strange baryons of particular interest to us here.

We discuss in the following, three classes of reactions which are the most relevant ones for the process of time evolution of strange particle abundances in the hot hadronic gas phase, viz. strangeness production, strangeness exchange, and antibaryon annihilation.

(a) For the case of strangeness production we assume the following reactions to be the most effective ones:

$$\pi + N \to \bar{K} + Y, \quad \pi + \bar{N} \to K + \bar{Y}, \quad \pi + \pi \to K + \bar{K}$$

$$\pi + Y \to \Xi + \bar{K}, \quad \pi + \bar{Y} \to K + \bar{\Xi}, \qquad (3.10)$$

$$\pi + \Xi \to \Omega + \bar{K}, \quad \pi + \bar{\Xi} \to K + \bar{\Omega},$$

[Y: hyperons Λ or Σ; $\bar{K} = q\bar{s}$ kaons (K^+, K^0)].

The common reaction feature of all processes listed here is the $q\bar{q} \to s\bar{s}$ reaction (see Figure 3.3) where several quarks are spectators and a $q,\bar{q}$ pair is annihilated and replaced in the final channel by an $s\bar{s}$ pair. We record the magnitude of the experimental value of the cross-section for the reaction

$$\pi + p \to Y + \bar{K} \quad (p \simeq \text{proton}),$$

which is about 0.1 mb in the energy region under interest, and infer therefrom that strangeness phase space saturation in HG should be a relatively slow process.

(b) It is also clear that in nuclear collisions, direct pair production of multiple-strangeness-carrying (anti-) baryons is strongly suppressed. But these particles may be readily produced by the following reactions making use of iterated strange-quark exchange:

$$K + N \to Y + \pi, \quad \bar{K} + \bar{N} \to \bar{Y} + \pi,$$

$$K + Y \to \Xi + \pi, \quad \bar{K} + \bar{Y} \to \bar{\Xi} + \pi, \qquad (3.11)$$

$$K + \Xi \to \Omega + \pi, \quad \bar{K} + \bar{\Omega} \to \bar{\Omega} + \pi.$$

The underlying type of a subprocess for all reactions in eq. (3.11) is depicted in Figure 3.4 where the strange quark from a kaon is exchanged to the baryon and forms a hyperon Y. We observe that all these reactions are 'exothermic', giving up energy, and therefore one finds for the reaction

$$K + N \to Y + \pi$$

an experimental cross-section (on average of the order of 1 mb), which is roughly ten times larger than the production cross-section. This means that strangeness is much faster redistributed over the strange-particle family than produced. This implies that the *relative* chemical equilibrium of s-quarks is established as soon as the s-quarks are produced during the lifetime of the fireball. One should further record that such exchange reactions proceed often via resonant intermediate states:

$$K + N \to Y_{res} \to Y + \pi.$$

In the framework of the present approach we will neglect to consider explicitly the existence of these resonances as the cross-sections we use include the effect of their presence. Consideration of the abundance evolution of intermediate resonances could possibly accelerate the approach to the *relative* chemical equilibrium. This, as discussed, is anyway already much faster

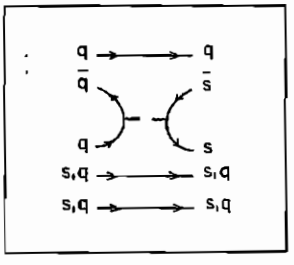

Figure 3.3 Typical quark flow diagram for strangeness production reaction: annihilation of a $q\bar{q}$-pair and production of an $s\bar{s}$-pair. Several quark spectator lines are also indicated.

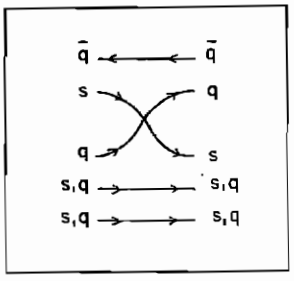

Figure 3.4 Typical quark flow diagram for strangeness exchange reaction: exchange of the s-quark from the initial K meson to the final baryon. Several quark spectator lines are also indicated.

than the approach to the absolute equilibrium, viz. the saturation of phase space. Hence, without altering any of the quantitative results, we may neglect the presence of intermediate renonances in the strangeness exchange channels, so much so that we use the cross-sections which incorporate such effects.

(c) Now one has to notice that the generation of strange antibaryons proceeds via the abundance of antinucleons which, however, should have a very low phase space density in the HG phase. This is a consequence of the low production cross-sections for $\bar{p}$ as well as of the strength of $p\bar{p}$ annihilations into multiple pion final states. Consider e.g. the annihilation reaction

$$p + \bar{p} \rightarrow 5\pi$$

cross-section which is approximately 100 times larger than the strangeness production cross-section via pions. Thus even though $\bar{p}$ phase space density (if saturated) is quite low (and the actual $\bar{p}$ abundance is still lower, as $\bar{p}$ are subject to a dynamical equilibrium), we also include the following set of annihilation reactions in our calculations as our primary concern is the strange antibaryon annihilation. In this work we have concentrated of the five-body final state because this channel is favoured by phase space considerations.

$$\begin{aligned} &N + \bar{N} \rightarrow \approx 5\pi, \\ &Y + \bar{N} \rightarrow K + \approx 4\pi, \qquad \bar{Y} + N \rightarrow \bar{K} + \approx 4\pi, \\ &\Xi + \bar{N} \rightarrow 2K + \approx 3\pi, \qquad \bar{\Xi} + N \rightarrow 2\bar{K} + \approx 3\pi, \\ &\Omega + \bar{N} \rightarrow 3K + \approx 2\pi, \qquad \bar{\Omega} + N \rightarrow 3\bar{K} + \approx 2\pi. \end{aligned} \tag{3.12}$$

Several further remarks concerning the details of our treatment of the annihilation reaction must be made here.

(i) In principle, we should include further annihilation channels between different kinds of baryons and antibaryons not listed in eq. (3.12). However, any other reaction would be further suppressed by both participants having a relatively small (equilibrium) phase space density.

(ii) We know from the study of $p\bar{p}$ annihilation that the multiple final pion channel proceeds, at least in part, via intermediate resonances. The issue at hand in HG phase is whether these resonances could induce reactions before their decay? We believe that the neglect of the intermediate resonance-induced processes leads to an overestimate of abundance of multistrange hadrons in HG.

(iii) As only a selection of all hadronic states has been mentioned in the eqs. (3.10), (3.11) and (3.12), one may wonder if the consideration of more massive resonances does not essentially influence our results: although the number densities of particles in statistical equilibrium become exponentially smaller with their increasing mass, the number of hadronic states also increases exponentially and both effects largely compensate each other (statistical bootstrap, ref. [1]). But a short-lived system such as formed in high-energy nuclear collisions will not be capable of populating such high-mass states unless a quark–gluon plasma state has been formed. Thus, in order to establish a comparison between QGP and HGP, we have to reject any massive resonances when working under the assumption of HGP only.

We now proceed to discuss the evolution equations for the densities of particles included in our time evolution calculations. We will study the quantitative time evolution of the densities. The evolution in space or momentum is discussed only qualitatively.

The momentum integrated time evolution equations take the general form [17]

$$\frac{\mathrm{d}}{\mathrm{d}t}\rho_i(t) = \sum_j \left\{ \langle \sigma_j v \rangle \prod_{l_j} \rho_{l_j}(t) \right\}_j - \text{inverse reactions}, \tag{3.13}$$

where the index i denotes π, K, Y, Ξ, Ω and their antiparticles (we do not distinguish different isospin states), and j sums over all reactions in which species i is produced. Index l_j denotes the particles (typically two) which participate in the production reaction in process j of the reaction (3.13).

The quantity $\langle \sigma_j v \rangle$ is the (thermal) averaged cross-section for an initial channel to lead to a specific final one which includes the particle i. In general we will treat two-body initial states and so we have

$$\langle \sigma^n_{ab} v_{ab} \rangle = \frac{\int \mathrm{d}^3P_a \, \mathrm{d}^3P_b \, f_a(P_a) \, f_b(P_b) \, \sigma^n_{ab} v_{ab}}{\int \mathrm{d}^3P_a \, \mathrm{d}^3P_b \, f_a(P_a) \, f_b(P_b)} \tag{3.14}$$

where $\sigma^n_{ab} v$ is the cross-section for the a + b $\rightarrow$ n-bodies process, v_{ab} the relative velocity of the incoming particles and $f_a(P_a)$, $f_b(P_b)$ their momentum distributions normalized such that

$$\int \mathrm{d}^3P_i \, f_i(P_i) = 1. \tag{3.15}$$

Use of the Boltzmann momentum distribution functions induces only in the case of pions inaccuracies at the level of 10% and requires further improvement.

In the evaluation of the statistical average $\langle \sigma v \rangle$ [eq. (3.14)] the threshold effect is encountered since σ is equal to zero unless the energy of the incoming channel in the centre-of-mass system is equal to or greater than the energy required for the final channel. This can be made explicit by writing σ in terms of T-matrix elements [18]:

$$\sigma^n_{ab} = F^{-1} \int \prod_i^n \mathrm{d}^4P_i \, \delta(P_i^2 - m_i^2) \, \theta(P_i^0) \, \delta^4\Big(P_a + P_b - \sum_i^n P_i\Big) \times |\langle f|T|i\rangle|^2 \tag{3.16}$$

where

$$F = 2\Big\{[s - (m_a + m_b)^2][s - (m_a - m_b)^2]\Big\}^{1/2} (2\pi)^{3n-4}. \tag{3.17}$$

In principle one should now proceed to calculate theoretically the transition probabilities

$$|M|^2 := |\langle f|T|i\rangle|^2, \tag{3.18}$$

but this is not a feasible proposition and a more phenomenological approach is adopted. In the case of measured cross-sections $\sigma_{ab}^{n}(s)$, a functional parameterization of the data, in dependence on the centre-of-mass energy $\sqrt{s}$ can be employed. After some algebra (which is outlined in ref. [17]), we obtain

$$\langle \sigma_{ab}^{u} v_{ab} \rangle = \frac{\beta}{4} \times \frac{\int_{\sqrt{s_0}}^{\infty} d\sqrt{s}\, \sigma(\sqrt{s})[s-(m_a+m_b)^2][s-(m_a-m_b)^2] K_1(\beta\sqrt{s})}{m_a^2 m_b^2 K_2(\beta m_a) K_2(\beta m_b)} \tag{3.19}$$

where $\sqrt{s_0}$ is the threshold denoting the lowest energy necessary to allow for the reaction in the centre-of-mass system of the two colliding particles under consideration. Experimental information is available for the following reactions:

(a) $\pi + p \rightarrow \bar{K} + Y$ 'strangeness production' (only charged pions)

(b) $K + p \rightarrow Y + \pi$ 'strangeness exchange' (only charged kaons)

(c) $p + \bar{p} \rightarrow 5\pi$ 'annihilation'

(More details about these reaction channels used and cross-section parameterization is contained in ref. [17].)

For each class of the above-mentioned subprocess one experimental cross-section is used in order to calculate the corresponding average, eq. (3.14). For the cases of reactions for which no experimental information is available, we assume that T-matrix elements contained in the expressions for the cross-sections are independent of the outgoing particle momenta and are nearly constant for the energy range considered. This assumption seems to be valid for low centre-of-mass energies in hadron–hadron reactions [18]. As a consequence of these assumptions (see ref. [17]),

$$\langle \sigma_{ab}^{n} v_{ab} \rangle = \frac{\beta}{4} \frac{|M(a+b \rightarrow n)|^2}{(2\pi)^{3n-3}} \times \frac{\int_{\sqrt{s_0}}^{\infty} d\sqrt{s}\, s I_2^{in} I_n^{out} K_1(\beta\sqrt{s})}{m_a^2 K_2(\beta m_a) m_b^2 K_2(\beta m_b)} \tag{3.20}$$

with

$$I_2^{in} = \left(\frac{\pi}{2}\right) s^{-1} \left\{ [s-(m_a+m_b)^2][s-(m_a-m_b)^2] \right\}^{1/2} \tag{3.21}$$

and

$$I_n^{out} = \int \prod_i^n d^4 P_i \delta(P_i^2 - m_i^2)\, \theta(P_i^0)\, \delta^4\Big(P - \sum_i^n P_i\Big) \tag{3.22}$$

the n-particle phase space of the outgoing particles.

We have now reduced the problem of calculating $\langle \sigma v \rangle$ to the knowledge of $|M|^2$. All mean thermal cross-sections are calculated according to the assumption of constant matrix elements $|M|^2$ and the reactions of each class of the three subprocesses considered are normalized to the one which we can gauge using the experimental input. Only phase space dependence in each individual class characterizes the different reactions. We further note that the matrix element $|M|^2$ for reactions where particles and antiparticles are interchanged, is the same, and further that the mean thermal cross-section of the reverse reactions is given by the forward reactions times the equilibrium constant which weights the equilibrium densities of the incoming particles by the outgoing ones. In the light of the above remarks, we have now established that three typical reaction cross-sections, viz 'strangeness production', 'strangeness exchange' and 'baryon annihilation', determine the parameters needed in the non-linear differential population evolution equations, eq. (3.13).

We still have to specify the initial values of all the densities at a given time t_0. We wish to compare here scenarios in which particle abundances are calculated as if the reactions were to proceed entirely either through HG of QGP phases. Thus the densities of strange particles at t_0 are all set equal to zero; we neglect direct strangeness production in the first moments of the collision. We will start with strange-particle production in HG at a time $t_0 = 1 \times 10^{-24}$ s since after that time the pion and nucleon densities should have reached approximately their equilibrium values [16]. For antinucleon density the chemical equilibrium value is assumed. But we record that the assumption of baryochemical equilibrium for antinucleons is likely to be a gross overestimate leading to an overestimation of abundance of strange antibaryons generated in the HG phase. One should further notice that a lower abundance of antinucleons would further lead to longer antistrange baryon equilibration time in HG than reported here.

The time evolution of the system described above is now fixed once the statistical parameters, viz. temperature T and baryon chemical potential μ_B, are prescribed. As mentioned, we assume T and μ_B to be space time independent while computing the characteristic times of equilibration and time-dependent particle abundances. These then can be folded, if needed, with the given space time distributions in particular applications not further pursued here.

3.3 Discussion of results for HG and QGP

We now discuss the numerical results for the expected strangeness abundance and compare the results for both possible phases.

In Figure 3.5 we show the time evolution of total strangeness density for both phases, i.e. the hadronic gas (HG) phase and the quark–gluon plasma (QGP) phase. The total strangeness for the HG phase is given by

$$\rho_s^{HG} = \rho_K^{HG} + \rho_Y^{HG} + 2\rho_\Xi^{HG} + 3\rho_\Omega^{HG}, \tag{3.23}$$

and due to exact strangeness conservation, is equal to the total antistrangeness $\rho_{\bar{s}}^{HG}$. When considering the curves of Figure 3.5, (ref. [17]), we see that after a typical break-up time of the HG of $\approx 5 \times 10^{-23}$ s, strangeness abundance expected in the HG phase is still about a factor of three smaller than the equilibrium value. If the hypothesis is made that this is the time of a nuclear collision independent of the

two phases reached, then one finds in nuclear collisions, $\rho_s^{QGP}/\rho_s^{HG} \approx 30$. This factor will be greatly amplified by considering highly strange objects, such as $\bar{\Omega}$ (see below).

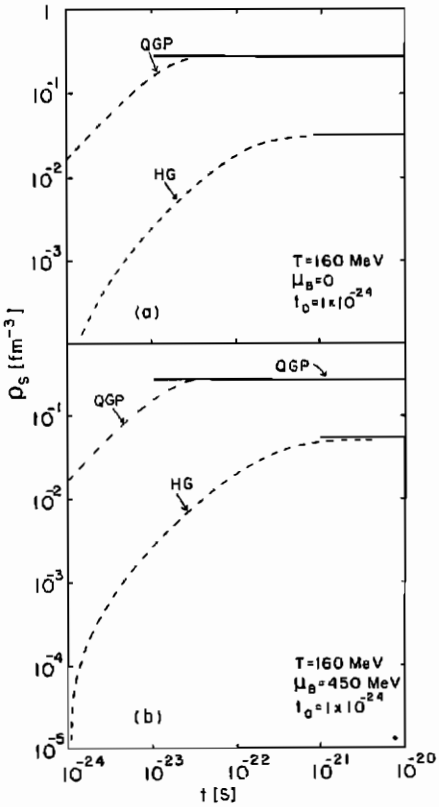

Figure 3.5 Time evolution of strange-quark densities in HG and QGP at a fixed temperature $T = 160$ MeV. (a) Baryochemical potential $\mu_B = 0$; (b) $\mu_B = 450$ MeV.

This ratio is quite sensitive to the lifetimes of HG and QGP phases and may still be larger, as the equilibration time for the non-strange HG matter is greater than 1×10^{-24} s. Furthermore, note that the relation between μ_B and baryonic density depends on the nature of the phase; our comparison is therefore indeed made at different baryonic densities: at the same value of μ_B QGP is very likely more compressed than HG.

We now turn to the discussion of the strange antibaryons. We find that the HG density of anti-omegas as well as omegas is a factor of $\approx 10^3$ lower than their equilibrium values for a break-up time between 10^{-23} and 10^{-22} s (see Figure 3.6). This is true for baryonless as well as for baryon-number-carrying hadronic gas (again see Figure 3.6).

Anticascades are suppressed by a factor of $\approx 10^2$ with respect to their equilibrium values. Hence, anti-omegas are 4 – 5 orders of magnitude below the plasma values (see vertical bar in Figure 3.6b). We emphasize that in more realistic calculations with expansion and cooling of the hadronic fireball taken into account and with a lower initial density of antinucleons than the equilibrium values taken here, one would, very likely, end up with an even lower density of strange antibaryons from HG. Hence, strange antibaryons appear as most promising characteristic signals for the detection of QGP.

We now briefly discuss the model used to estimate particle yields in quark–gluon plasma shown in Figures 3.6b and 3.6c. Very little is known theoretically about hadron production from QGP, but one may hope that in the case of baryon or antibaryon production a simple 'combinatoric' break-up picture as suggested by Biro and Zimanyi [19] might provide an order-of-magnitude estimate. In the framework of this model the available quarks are distributed among the final-state hadrons by using two constant probabilities, one for meson production and one for baryon

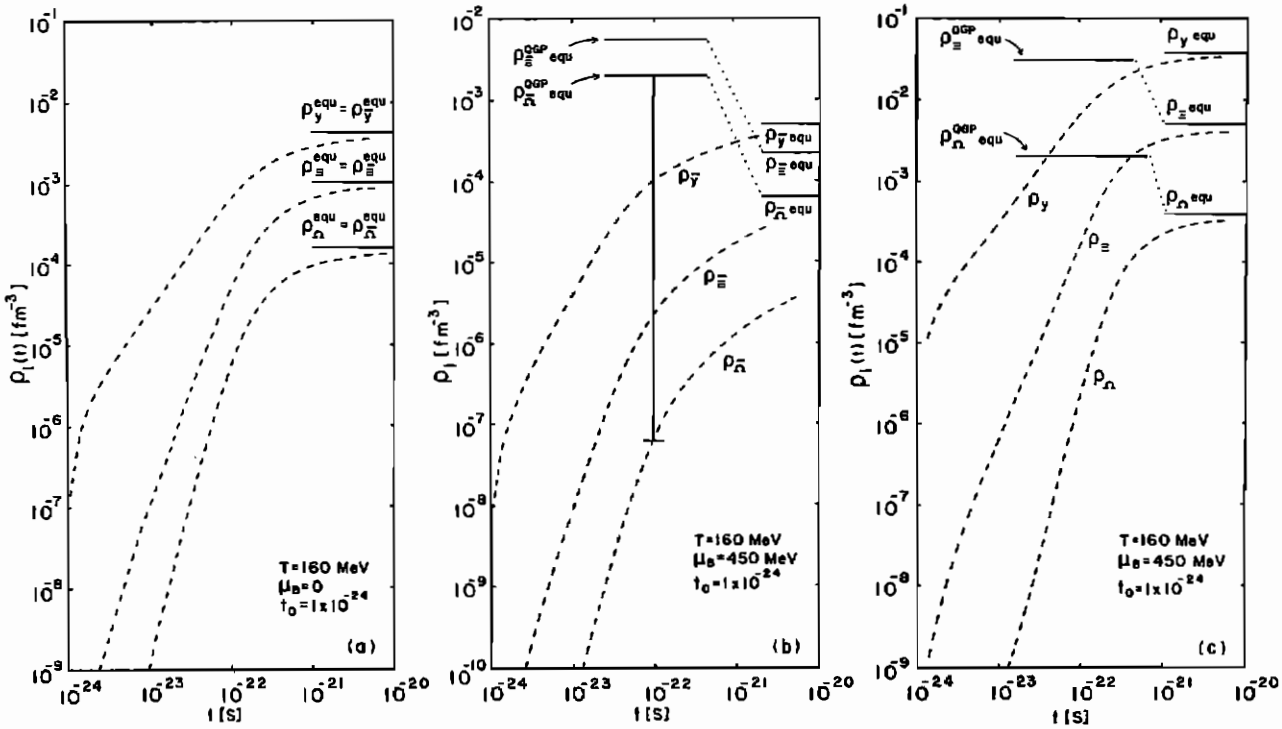

Figure 3.6 Approach to equilibrium of various strange-particle densities in HG phase at fixed $T = 160$ MeV. (a) $\mu_B = 0$; (b) and (c) $\mu_B = 450$ MeV. QGP combinatoric model results are shown in (b) and (c).

production. In particular, the abundance of mesons is assumed to be related to quark abundances by

$$\rho_{\bar{K}} = \alpha\rho_q\rho_{\bar{s}} \tag{3.24a}$$

$$\rho_K = \alpha\rho_{\bar{q}}\rho_s \tag{3.24b}$$

$$\rho_\pi = \alpha\rho_q\rho_{\bar{q}} \tag{3.24c}$$

where α is a recombination constant. The abundance of baryons is similarly given by

$$\rho_N = \frac{\beta}{3!}\rho_q^3; \quad \rho_{\bar{N}} = \frac{\beta}{3!}\rho_{\bar{q}}^3 \tag{3.25a}$$

$$\rho_Y = \frac{\beta}{2!}\rho_q^2\rho_s; \quad \rho_{\bar{Y}} = \frac{\beta}{2!}\rho_{\bar{q}}^2\rho_{\bar{s}} \tag{3.25b}$$

$$\rho_\Xi = \frac{\beta}{2!}\rho_q\rho_s^2; \quad \rho_{\bar{\Xi}} = \frac{\beta}{2!}\rho_{\bar{q}}\rho_{\bar{s}}^2 \tag{3.25c}$$

$$\rho_\Omega = \frac{\beta}{3!}\rho_s^3; \quad \rho_{\bar{\Omega}} = \frac{\beta}{3!}\rho_{\bar{s}}^3. \tag{3.25d}$$

As each gluon is in principle equivalent to a virtual $q-\bar{q}$ pair, gluon abundances could contribute to the above equations. In this first estimate, the influence of gluon fragmentation is ignored. The different quarks are redistributed between hadrons subject to the conservation laws:

$$\rho_s = \rho_K + \rho_Y + 2\rho_\Xi + 3\rho_\Omega \tag{3.26a}$$

$$\rho_{\bar{s}} = \rho_{\bar{K}} + \rho_{\bar{Y}} + 2\rho_{\bar{\Xi}} + 3\rho_{\bar{\Omega}} \tag{3.26b}$$

$$\rho_q = \rho_\pi + \rho_{\bar{K}} + 3\rho_N + 2\rho_Y + \rho_\Xi \tag{3.26c}$$

$$\rho_{\bar{q}} = \rho_\pi + \rho_K + 3\rho_{\bar{N}} + 2\rho_{\bar{Y}} + \rho_{\bar{\Xi}} \tag{3.26d}$$

and further subject to the condition that $\rho_s - \rho_{\bar{s}} = 0$. For the two parameters α and β we find

$$\alpha = \frac{(\rho_s+\rho_q)^2-(\rho_s+\rho_{\bar{q}})^2}{\rho_q(\rho_q+\rho_s)^2-\rho_{\bar{q}}(\rho_{\bar{q}}+\rho_{\bar{s}})^2} \tag{3.27a}$$

$$\beta = \frac{2(\rho_q-\rho_{\bar{q}})}{\rho_q(\rho_q+\rho_s)^2-\rho_{\bar{q}}(\rho_{\bar{q}}+\rho_{\bar{s}})^2} \tag{3.27b}$$

where all q, $\bar{q}$ and $s = \bar{s}$ abundances can be assumed to be given by their respective equilibrium values in the QGP where Boltzmann statistics was used for the s, $\bar{s}$ and $\bar{q}$ quarks.

$$\rho_s = \rho_{\bar{s}} \simeq \frac{3T^3}{\pi^2}\left(\frac{m_s}{T}\right)K_2\left(\frac{m_s}{T}\right) \tag{3.28a}$$

$$\rho_{\bar{q}} \simeq \frac{6T^3}{\pi^2}e^{-\mu_B/3T} \tag{3.28b}$$

$$\rho_q - \rho_{\bar{q}} = \frac{T^3}{\pi^2}\left\{\left(\frac{\mu_B}{3T}\right)^3+\pi^2\left(\frac{\mu_B}{3T}\right)\right\} \tag{3.28c}$$

and

$$\rho_q = \rho_{\bar{q}}\left[\frac{\rho_q-\rho_{\bar{q}}}{\rho_{\bar{q}}}+1\right] \tag{3.28d}$$

4. State of chemical equilibration in hadronic reactions

We have, by now, largely settled the theoretical framework for analysing strange-particle abundances in both possible phases of hadronic matter. We have shown that the dynamical approach of the abundance to the maximum available phase space density is an essential cornerstone of the study of both phases of hadronic matter. In this section we intend to show that hadronic collisions at high centre-of-mass energies show a degree of chemical equilibration among strange particles which cannot be achieved in a phase in which the process of chemical equilibration is based on reactions between individual hadrons.

Let us turn first to p–p and p–nucleus experiments [20] where the data were analysed in the framework of a chemical equlibrium hadronic gas model [21]. Since we want to describe different particle multiplicities, including the rapidity distribution of the baryon number, it is necessary to find for the baryochemical potential μ_B, controlling the baryon number, a distribution between the central and projectile rapidity regions. In ref. [21] the linear relationship

$$|x|m_N = \mu_B \tag{4.1}$$

has been proposed, with x as the usual Feynman variable, which is the fraction of the maximum momentum that a particle could carry. $m_N = 940$ MeV is the nucleon mass.

The physics underlying this approach is the hypothesis that in p–p collisions the valence quarks of one nucleon largely penetrate the other nucleon rather freely without much interaction, while much of the energy and momentum in the gluon field remains in the central reaction region. This region, therefore, should exhibit zero net baryon and charge number whereas in the maximum rapidity region we would expect to see the quantum numbers of the incoming particles; that is, the baryon number is found mainly in the projectile (and target) fragmentation regions. A dynamical relation between x and μ_B fulfilling these requirements is given by eq. (4.1) — for $x = \pm 1$ (projectile/target region) we have $\mu_B \to m_N$ and for $x = 0$ (central region) we have $\mu_B = 0$.

In order to calculate strange-particle abundances, we follow here the approach of ref. [21] which is an extension of the model outlined in section 3.1 by incorporating, aside from baryon number (B) and strangeness (s), the conservation of the electric charge (Q). This is necessary in the light of experimental data and the need to distinguish up and down quarks.

Following the approach outlined in section 3.1 we find for the singly strange particles.

$$\langle n_{K^+}\rangle/\langle n_{K^-}\rangle = \lambda_Q^2\lambda_s^{-2} \tag{4.2a}$$

$$\langle n_{\bar{\Lambda}} + n_{\bar{\Sigma}^0}\rangle/\langle n_\Lambda + n_{\Sigma^0}\rangle = \lambda_B^{-2}\lambda_s^{-2} \tag{4.2b}$$

$$\langle n_{\bar{\Sigma}^\pm}\rangle/\langle n_{\Sigma^\pm}\rangle = \lambda_B^{-2}\lambda_s^{-2}\lambda_Q^{\pm 2}. \tag{4.2c}$$

λ_s by itself is a function of λ_B and λ_Q [compare eq. (3.5)]. The measured π^+/π^- ratio is first used in order to fix λ_Q which

describes the up–down quark asymmetry, since

$$\pi^+/\pi^- \simeq \lambda_Q^2. \tag{4.3}$$

The experimental data for pp reactions can be satisfactorily represented by the functional form

$$\lambda_Q^2 = \pi^+/\pi^- = \exp(2x) \tag{4.4}$$

in the region $0.2 \leq x \leq 0.7$.

The assumption (4.1) implies, in turn,

$$\lambda_B^2 = e^{2\mu_B/T} = e^{2xm_N/T} \tag{4.5}$$

$$= \exp(10x); \quad T = 175 \text{ MeV: pp reactions}$$

$$= \exp(12.5x); \quad T = 150 \text{ MeV: pN reactions}$$

where, as indicated, the temperature parameter T was taken to be 175 MeV for p–p collisions and 150 MeV for p–N reactions in agreement with values deducible from mean transversal momenta of mesons [22]. As λ_B^2 changes between pp and pN reactions, we will also change λ_Q^2 to $\exp(2.2x)$ for pN reactions.

In Figure 4.1 we display the calculated and measured particle ratios. Especially the double ratio $(\bar{p}/p)/(\pi^-/\pi^+)$ which is equal to λ_B^{-2} and therefore provides an independent consistency check for the assumed important relation (4.1), gives a satisfactory agreement with the data (Figure 4.1d). Taking any other power of x would destroy the visible exponential behaviour of this double ratio as a function of x.

Consider now the measured multistrange antiparticle to particle ratios [21]. The comparison with the data of Bourquin et al. [20g] is shown in Figure 4.2 where the predictions are indicated by filled circles. As a function of strangeness (s = 1, 2, 3), the data are relatively well described by relative abundances obtained in the framework of the hadronic gas model.

Even more surprising is the fact that the total mean multiplicities of antistrange hyperons as deduced in ref. [20g] are compatible with the abundances we would get from a hadronic gas in chemical equilibrium at a temperature of

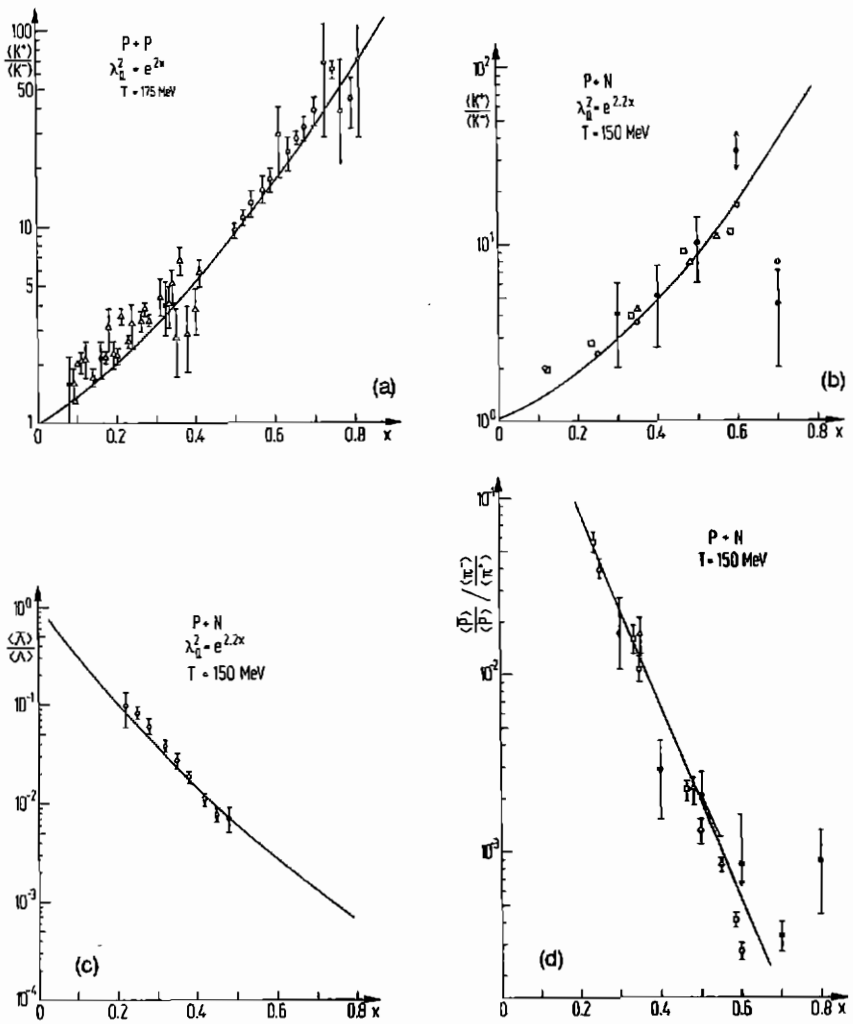

Figure 4.1 Particle abundance ratios as function of x in pp and pN collisions. Drawn lines are our calculated results with $T^{(pp)} = 175$ MeV and $\lambda_B^{(pp)} = \exp(2x)$ or $\lambda_B^{(pN)} = \exp(2.2x)$ and $T^{(pN)} = 150$ MeV. (a) K^+/K^-(pp): ref. [20b] (△); ref. [20c] (●); ref. [20d] (○). Data averaged over range of transverse momenta and $\sqrt{s}$. (b) K^+/K^-(pBe): ref. [20e] (○, at $p_{proj} = 200$ GeV/c; ref. [20f] (○, at $p_{proj} = 300$ GeV/c); ref. [20g] (△, pBeO at $p_{proj} = 210$ GeV/c); ref. [20g] (●, pA different A, $p_{proj} = 100$ GeV/c). (c) $(\bar{\Lambda} + \Sigma^0)$ pBe, ref. [20h]. (d) Double ratio $(\bar{p}/p) : (\pi^-/\pi^+)$, refs. [20f–h].

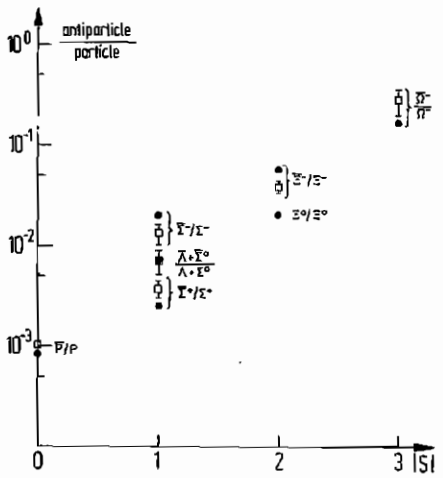

Figure 4.2 Antibaryon to baryon ratio for p-Be collision as function of strangeness s for $x = 0.48$, ref. [20g]. Our calculated points are indicated by a filled circle [$T = 150$ MeV, $\lambda_Q = \exp(2.2x)$].

150 MeV and a volume of about 1 fm^3, when further assuming that these particles are mainly produced in the central region of rapidity where $\mu_B = 0$. However, from our 'approach to equilibrium' analysis in the previous section, we know that only less than one promille of the phase space abundance is excited by reactions in the hadron gas phase. Further, we note that the $\bar{\Omega}$ abundance seen would require an active gas volume of $\approx 10^4$ fm^3 in order to be generated in the hadronic gas phase during the reaction time 10^{-23} s. Thus, we can conclude that the relatively high abundance of antistrange hyperons has not been produced by hadronic gas reactions and that it therefore must originate from reactions between quarks and gluons.

Consider, as a further example of this argument, the relatively large number of anti-protons produced in p–p collisions [20a, b, c]. They are produced mainly in the central rapidity region where we expect zero baryon number and where particles carry only relatively low longitudinal momenta. In the framework of the chemical equilibrium hadron gas model we expect in this region of the abundance of antiprotons,

$$\langle n_{\bar{p}} \rangle = 2 \frac{VT^3}{2\pi^2} \left(\frac{m_N}{T}\right)^2 K_2\left(\frac{m_N}{T}\right) \qquad (4.5)$$

where Boltzmann statistics were used.

Adopting 160 MeV as the maximal temperature [1] for the hadronic gas phase we would need a volume of about 40 fm^3 for the hadronic gas in order to fit the high-energy ISR $\bar{p}$ data. This already seems to be a very large volume and we have not yet considered that antinucleons could not have saturated the available phase space during a collision lasting about $\tau \sim 10^{-23}$ s.

Again we see that either non-realistic assumptions about the size of hadronic gas volume or length of collision time must be made in order to describe the data in a conventional hadronic statistical model. We find that experiments with high energetic p–p as well as p–N collisions indicate a state of chemical equilibration which should not be achieved if the approach to equilibrium had succeeded through a series of collisions of individual hadrons only. The only resolution of this conflict is to assume that an intermediate state carrying the main characteristics of quark–gluon matter has been formed.

Our argument would not be consistent, though, if particle spectra did not have transverse momentum distributions corresponding to a high degree of thermalization, and in particular, a temperature of about 160 MeV [1]. In view of our hypothesis we now question: are the particle abundances and spectra compatible with a statistical system of thermalized quark–gluon matter, perhaps not in a state of perfect chemical equilibrium? (The latter remark is made in view of the short reaction time of the collision process in hadronic interactions, which we assume to be $\approx 2 - 4 \times 10^{-24}$ s in accordance with estimates based on experiments in p–p collisions and π-nucleus collisions [22].)

This question can be answered in the affirmative given a number of further observations. Recent experimental analysis of strange-quark production [23], including resonance decays, gives an s/q-ratio of about 0.2 at $\sqrt{s} \simeq 23$ GeV, whereas our non-equilibrium prediction for quark–gluon matter at $t_{\text{break-up}} \approx 2 - 4 \times 10^{-24}$ s is about 0.1 at a temperature of $T = 160$ MeV. We further notice that higher temperatures, or longer reaction times, tend to result in a larger s/q ratio. Hence there is qualitative, even if not quantitative, agreement with experiment. In contrast to this, in the hadronic gas at $T = 160$ MeV and at the same break-up time, a value of the relative abundance is obtained, which is about a factor of 100 times smaller than the value extracted from data.

Similarly convincing is the fact that the abundance ratios K^+/π^+ and K^-/π^- approach the value of 0.4 for *low* $P_\perp$ jets at ISR energies of $\sqrt{s} \approx 45 - 62$ GeV, as shown in Figure 4.3a. Recent calculations [24] show that the K^+/π^+ ratio one expects from a quark–gluon plasma (see Figure 4.3b) assumes a similar value.

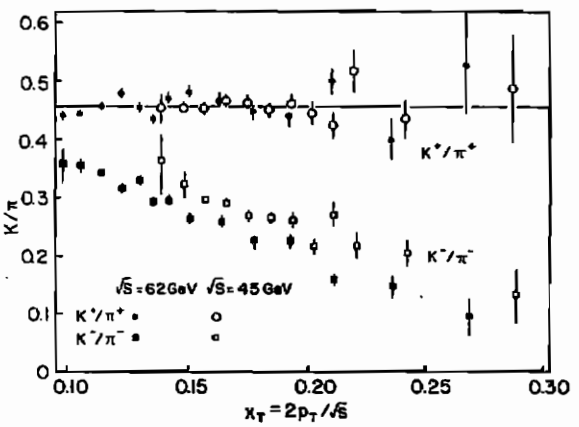

Figure 4.3a Cross-section ratios measured at the ISR as function of x_T for $d\sigma(K^+)/d\sigma(\pi^+)$ and $d\sigma(K^-)/d\sigma(\pi^-)$. SFM collaboration (1984). The approximate equality of the ratios at small x reflects $s\bar{s}$ production out of the vacuum and lack of K^- rescattering.

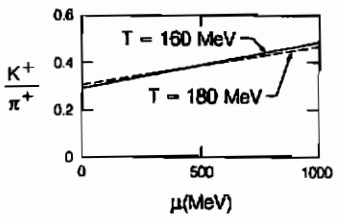

Figure 4.3b Ratio of K^+/π^+ expected from quark–gluon plasma [24].

Our present discussion is not restricted to high-energy reactions, as seen, considering $\bar{p}$–d → strangeness annihilations which also confirm our considerations quantitatively. Assume [25] that when *slow* antiprotons penetrate into a nucleus (of course with a small probability), the first step in the annihilation process will be the formation of a baryon-number zero fireball, filled with coloured gluons and quark–antiquark pairs. As it turns out, this picture allows a satisfactory description of the π-multiplicities in annihilations where it is important to consider the conservation of isospin [26]. In $\bar{p}$N reactions such a state would then break up into several mesons, a process that may last sufficiently long to allow the fireball to sometimes collide with one or more of the nearby nucleons in a nucleus. Very likely, this will lead to the absorptions of some number A of nucleons into the quark (gluon) fireball. Such a quark droplet will ultimately disintegrate into $A - 1$ baryons and several mesons. We should expect a significant enhancement of the strange-particle abundance in such a fireball. An experiment to observe a plasma droplet could employ a strangeness trigger. In Figure 4.4 we show the recoil nucleon spectrum in the $\bar{p}$–d annihilation when the reaction is accompanied by $K\bar{K}$ production [27]. Indeed, a strong enhancement at proton momenta $p_\perp > 0.3$ GeV with a $T = 160$ MeV slope is seen. It is very interesting to note that this effect apparently fades in the background when the $K\bar{K}$ trigger is not used (see Figure 2 of ref. [28]). Another confirmation of quark fireball interpretation of the $\bar{p}$d reaction triggered by strangeness formation is obtained by considering the reaction

$$\bar{p}d \rightarrow \Lambda + X. \tag{4.9}$$

The strangeness is now attached to the nucleon and the reaction is self-analysing in the sense that the recoiling particle — Λ — has the trigger quantum number. Indeed, Oh and Smith [29] recorded that the transverse momentum Λ spectrum is identical to their p spectrum in the bump above $p_\perp > 0.3$ GeV. Along with more recent measurements of the reaction (4.9) [30] an alternative interpretation in terms of $\bar{K}$-exchange was attempted which, however, seems to fall short of the data. Experimental evidence against the $\bar{K}$-exchange mechanism is the anomalous enhancement of 'K–d reactions' when the spectator momentum exceeds 200 MeV/c [31]. In favour of our present interpretation is the recent theoretical result that surface radiation of hot hadronic gas with conserved charge and strangeness on the surface of a hot droplet leads quantitatively to the observed momentum distribution and absolute normalization for the $\bar{p}$–d spectator spectrum [32]. We thus draw from all this the conclusion that strangeness appears to be a valid trigger for those $\bar{p}$–d reactions which proceed through an intermediate compound fireball state — a quark–gluon droplet of nearly 3 GeV mass and baryon number 1.

Finally, we briefly consider the available sparse data on strange-particle production in nucleus–nucleus collisions at 1.8–2.1 GeV/A. It turns out [33] that these data cannot be described by hadronic gas phase space saturated particle abundances. The conclusion one might draw here is that at these low nuclear energies strange-particle production is still dominated by reaction processes between individual hadrons, which therefore lead to particle abundances far below phase space saturation for hadronic gas models, as no quark matter has been formed which would have facilitated

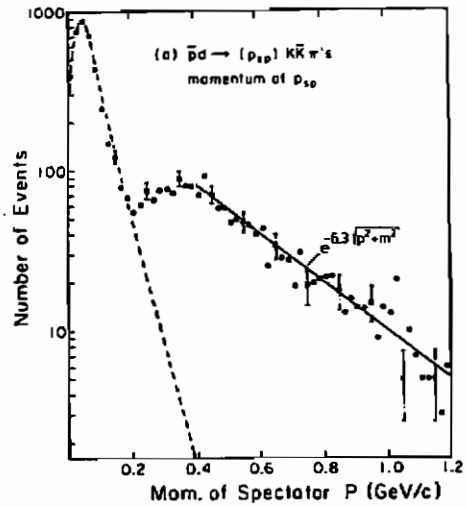

Figure 4.4 Momentum distribution of spectator protons in coincidence with strangeness production in $\bar{p}$d annihilations.

strangeness abundance formation. However, even in these reactions it is found that abundance ratios of strange particles follow the relative chemical equilibrium — that is, strangeness generated is rapidly redistributed among the final-state hadrons [33a].

5. Discussion and Conclusion

We have presented a number of arguments demonstrating the presence of a transitionary state of QCD colour degrees of freedom in various hadron–hadron as well as hadron–nucleus collision. In particular, the question of *why* the reaction products display such a high degree of thermal and chemical equilibration could be qualitatively and plausibly explained by this hypothesis, founding a working base for statistical models [1].

Assuming a reaction mechanism dominated by the large gluon–gluon abundances in a state of hadronic matter where the intrinsic colour degrees of freedom of the quarks and gluons are the underlying components of the reaction processes, we showed that even at very short times, i.e. about $2 - 4 \times 10^{-24}$ s, strange quarks, in particular, can reach the level of strangeness abundance we expect from a *hadronic gas*. We have shown that this is *not* the case for a reaction which proceeds through collisions between individual hadrons and where the colour degrees of freedom are practically frozen. Therefore the ultimate degree of equilibration in hadronic reactions is controlled by the achieved degree of melting of the hadronic vacuum. The excitation of colour degrees of freedom controls the degree of randomization and chemical equilibration at the end of the hadronic reaction.

The examination of high-energy p–p and p–N and even $\bar{p}$–d data with respect to antistrange quarks carrying hadrons lead to a confirmation of our collision picture. On the other hand, we noticed that nucleus–nucleus collisions at 1.8–2.1 GeV/A are still dominated by the collisions between individual hadrons, which means that vacuum melting had not been possible at these energies. In the light of our study of the pN reactions [21], we expect that this situation will change when, in the near future, higher energetic beams for nuclear collisions become available at CERN-SPS and we

are able to obtain larger regions of melted vacuum in space and time, as we can today in pp and pN collisions. The abundance of strange hadrons produced by the transitionary existence of such a quark–gluon plasma should be well above the abundance we observe now.

In the final process of hadronization of the quark–gluon state, the overabundance of strangeness, as produced in the quark–gluon plasma state, can be diluted by final hadron gas expansion and final-state reactions. Therefore, strangeness abundance may approach (from above) the abundance characteristic of the hadronic gas, a level which cannot be reached otherwise by a reaction which relies on the scattering between individual hadrons. Thus it is the approach to the hadronic gas equilibrium abundances which distinguishes between the two phases; abundances of particles like $\bar{\Lambda}$, $\bar{\Xi}$ and $\bar{\Omega}$ above or even at the level expected from the hadronic gas equilibrium considerations will prove the existence of a transitory state of quark–gluon plasma formed in nuclear collisions. Our theoretical calculations show that without the existence of such an intermediate quark–gluon plasma state, the hadronic gas strange-particle phase space cannot be properly populated during the short nuclear-collision time.

References

[1] (a) R. Hagedorn, Suppl. Nuovo Cimento **3** (1965) 147; **6** (1968) 311; (b) R. Hagedorn and J. Ranft, Suppl. Nuovo Cimento **6** (1968) 169; (c) R. Hagedorn, I. Montvay and J. Rafelski, Hadronic Matter at Extreme Energy Density, ed. N. Cabbibo (Plenum, New York, 1980)

[2] For further references and historical developments see: R. Hagedorn, How to get to QCD Matter from the Hadron Side by Trial and Error, Springer Lecture Notes in Physics **221** (1985) 53 (Proceedings, Helsinki Conference 'Quark Matter 1984') and CERN-preprint TH.3918/84

[3] L. van Hove and S. Pokorski, Nucl. Phys. B **86** (1975) 243

[4] R. Hagedorn, Riv. Nuovo Cim. **6** (1983) 1

[5] J. Rafelski and B. Müller, Phys. Rev. Lett. **48** (1982) 1066

[6] H.-Th. Elze, J. Rafelski and W. Greiner, Phys. Lett. B **124** (1983) 515 and Z. Phys. C **24** (1984) 361

[7] For an overview over the field of Lattice Monte Carlo Calculations see contributions to Proceedings of the Third International Conference on 'Ultra-Relativistic Nucleus–Nucleus Collisions', Brookhaven National Laboratory, Nucl. Phys. A **418** (1984) 447c; and Proceedings of the Fourth International Conference on Ultra-Relativistic Nucleus–Nucleus Collisions, 'Quark Matter '84', ed. K. Kajantie, in Springer Lecture Notes in Physics **221** (1985) 17

[8] (a) J. Rafelski, Extreme States of Nuclear Matter in the proceedings of the Workshop on Future Relativistic Heavy Ion Experiments, eds. R. Stock and R. Bock, GSI 81-6, and Universität Frankfurt Preprint UFTP 52/1981; (b) J. Rafelski, Phys. Rep. **88** (1982) 331; (c) J. Rafelski, 'Strangeness in Quark–Gluon Plasma', Universität Frankfurt, preprint UFTP 86/1982 and S. Afr. J. Phys. **6** (1983) 37; (d) J. Rafelski, Nucl. Phys. A **418** (1984) 215c

[9] (a) J.W. Harris, A. Sandoval, R. Stock, H. Stroebele, R.E. Renfordt, J.V. Geaga, H.G. Pugh, L.S. Schroeder, K.L. Wolf and A. Dacal, Phys. Rev. Lett. **47** (1981) 229; (b) S. Schnetzer et al., Phys. Rev. Lett. **49** (1982) 989; (c) A. Shor, K. Garezer, J. Caroll, G. Igo, J. Geaga, S. Abachi, A. Sagle, T. Mulera, V. Perez-Mendez, P. Lindstrom, F. Zarbakhsh and D. Woodward; Phys. Rev. Lett. **48** (1982) 1597; (d) M. Anikina, V. Aksinenko, E. Devientiev, M. Gazdzicki, N. Glagoleva, A. Golokhvastov, L. Goucharova, A. Grachov, K. Iovchev, S. Kadykova, N. Kaminsky, S. Khorozov, E. Kuznefsova, J. Lukstins, A. Matyushin, V. Matyushin, E. Okonov, T. Ostanevich, E. Shevchenko, S. Sidorin, G. Vardenga, O. Balea, N. Nikorovich, T. Ponta, L. Chikaidze, T. Dzobava, M. Despotashvili, I. Tuliani, E. Khusainov, N. Nurgozin, B. Suleimanov, E. Skrzypzak and T. Tymieniecka, Z. Phys. C **25** (1984) 1

[10] (a) A.T.M. Aerts and J. Rafelski, Strange Hadrons in the MIT Bag Model, UCT-TP 27/85 and CERN TH 4160/85; (b) L.J. Reinders and H.R. Rubinstein, Phys. Lett. B **145** (1984) 108; (c) S. Narison and E. de Rafael, Phys. Lett. B **103** (1981) 57; (d) J. Gasser and H. Leutwyler, Phys. Rep. **87** (1982) 77; (e) A.T.M. Aerts and J. Rafelski, Phys. Lett. B **148** (1984) 337

[11] (a) J. Rafelski and M. Danos, Nuclear Matter Under Extreme Conditions, UCT-TP 8/84, in Springer Tracts in Physics **231** (1985) 362; (b) M. Danos and J. Rafelski, Baryon-rich Quark–Gluon Plasma in Nuclear Collisions, UCT-TP 7/84

[12] (a) B.L. Combridge, Nucl. Phys. B **151** (1979) 429; (b) B.L. Combridge, J. Kripfganz and J. Ranft, Phys. Lett. B **70** (1977) 234

[13] P. Koch, Diploma Thesis, Frankfurt 1983 (unpublished)

[14] K. Redlich, Z. Phys. C **27** (1985) 633

[15] J. Rafelski, Strangeness and Phase Changes in Hadronic Matter, CERN-preprint TH.3685 (1983), appeared in LBL-12281, UC-34C, CONF-830675 (1983) p.489, proceedings of the 6th High Energy Heavy Ion Study at LBL, ed. H. Pugh

[16] A.Z. Mekjian, Nucl. Phys. A **384** (1982) 492

[17] P. Koch and J. Rafelski, Time Evolution of Strange Particle Densities in Hot Hadronic Matter, UCT-TP 26/84; Nucl. Phys. A **444** (1985) 678

[18] K. Kajantie and E. Byckling, Particle Kinematics (Wiley and Sons, 1973)

[19] T.S. Biro and J. Zimanyi, Nucl. Phys. A **395** (1983) 525

[20] (a) P. Capiluppi, G. Giacomelli, A.M. Rossi, G. Vannini and A. Bussiere, Nucl. Phys. B **70** (1974) 1; (b) P. Capiluppi, G. Giacomelli, A.M. Rossi, G. Vannini, A. Bertin, A. Bussiere and R.J. Ellis, Nucl. Phys. B **79** (1979) 189; (c) A.M. Rossi, G. Vannini, A. Bussiere, E. Albini, D. D'Alessandro and G. Giacomelli, Nucl. Phys. B **84** (1975) 269; (d) J. Singh, M.G. Albrow, D.P. Barber, P. Benz, B. Bosnjakovic, C.Y. Chang, A.B. Clegg, F.C. Erne, P. Kooijman, F.K. Loebinger, N.A. McCubbin, P.G. Murphy, A. Rudge, J.C. Sens, A.L. Sessoins and J. Timmer, Nucl. Phys. B **140** (1978) 189; (e) W.F. Baker, A.S. Carroll, I.-H. Chiang, D.P. Eartly, O. Fackley, G. Giacomelli, P.F.M. Koehler, T.F. Kycia, K.K. Li, P.O. Mazur, P.M. Mockett, K.P. Pretzl, S.M. Pruss, D.C. Rahm, R. Rubinstein and A.A. Wehmann, Nucl. Phys. B **51** (1974) 303; (f) D.S. Barton, G.W. Brandenburg, W. Busza, T. Dobrowolski, J.I. Friedman, C. Halliwell. H.W. Kendall, T. Lyons, B. Nelson, L. Rosenson, R. Verdier, M.T. Chiavodia, C. De Marto, C. Favuzzi, G. Germinario, L. Guerriero, P. La Vopa, G. Maggi, F. Posa, G. Selvaggi, P. Spinelli, F. Waldro, D. Cutts, R.S. Dulude, B.W. Hughlock, R.E. Lanou Jr., J.T. Massimo, A.E. Breuner, D.C. Carey, J.E. Elias, P.H. Garbincius, V.A. Polychronakos, J. Nassalski and T. Siemiarszuk, Phys. Rev. D **27** (1983) 2580; (g) M. Bourquin, R.M. Brown, Y. Chatelus, J.C. Chollet, M. Croissiaux, A. Degre, M. Ferro-Luzzi, D. Froidevaux, A.R. Fyfe, J.-M. Gaillard, C.N.P. Gee, W.M. Gibson, R.J. Gray, P. Igo-Kemenes, P.W. Jeffreys, B. Merkel, R. Morland, R.J. Ott, H. Plothow, J.-P. Repellin, B.J. Saunders, G. Sauvage, B. Schiby, H.W. Siebert, V.J. Smith, K.-P. Streit, R. Strub, J.J. Thresher and J. Trischuk, Nucl. Phys. B **153** (1979) 13; M. Bourquin, R.M. Brown, Y. Chatelus, J.C. Chollet, A. Degre, D. Froidevaux, A.R. Fyfe, J.-M. Gaillard, C.N.P. Gee, W.M. Gibson, P. Igo-Kemenes, P.W. Jeffreys, B. Merkel, R. Morand, H. Plothow, J.-P. Repellin, B.J. Saunders, G. Sauvagem, B. Schiby, H.W. Siebert, V.J. Smith, K.-P. Streit, R. Strub, J.J. Thresher and S.N. Tovey, Z. Phys. C **5** (1980) 275; (h) P. Scubic, O.E. Overseth, K. Heller, M. Scheaff, L. Pondrom, P. Martin, R. March, P. Yamin, L. Schachinger, J. Noran, R.T. Edwards, B. Edelman and T. Devlin, Phys. Rev. D **18** (1978) 3115

[21] W. Greiner, P. Koch and J. Rafelski, Phys. Lett. B **145** (1985) 142

[22] (a) L.J. Gutay et al., Phys. Rev. Lett. **37** (1976) 468; (b) A.T.

Loasanen et al., Phys. Rev. Lett. **38** (1977) 1; (c) C. Ezell et al., Phys. Rev. Lett. **38** (1977) 873
[23] T. Mueller, CERN-preprint EP 83-141 (1983)
[24] N.K. Glendenning and J. Rafelski, Phys. Rev. C **31** (1985) 823
[25] (a) J. Rafelski, Phys. Lett. B **91** (1980) 281; (b) J. Rafelski, Quark–Gluon Plasma in $\bar{p}$-Annihilation on Nuclei, UF-TP preprint 76/1982; in Proceedings of Workshop on Physics at LEAR, Erice, May 1982
[26] B. Müller and J. Rafelski, Phys. Lett. B **116** (1982) 274
[27] B.Y. Oh, P.S. Eastman, Z. Ming Ma, D.L. Parker, G.A. Smith and R.J. Sprafka, Nucl. Phys. B **51** (1973) 57
[28] P.S. Eastman, Z. Ming Ma, B.Y. Oh, D.L. Parker, G.A. Smith and R.J. Sprafka, Nucl. Phys. B **51** (1973) 29
[29] B.Y. Oh and G.A. Smith, Nucl. Phys. B **40** (1972) 151
[30] M.A. Mandelkern, L.R. Price, J. Schulz and D.W. Smith, Phys. Rev. D **27** (1983) 19
[31] O. Braun, V. Hepp, H. Stroebele and W. Witteck, Nucl. Phys. B **160** (1979) 467
[32] Ch. Derret, H.-Th. Elze, W. Greiner and J. Rafelski, Phys. Rev. C **31** (1985) 1360
[33] (a) P. Koch, J. Rafelski and W. Greiner, Phys. Lett. B **123** (1983) 151; (b) F. Asai, H. Sato and M. Sano, Phys. Lett. B **98** (1981) 19; (c) F. Asai and M. Sano, Prog. Theor. Phys. **66** (1981) 251; (d) C.M. Ko, Phys. Rev. C **23** (1981) 2760; (e) F. Asai, Nucl. Phys. A **365** (1981) 519; (f) F. Asai, H. Bando and M. Sano, Phys. Lett. B **145** (1984) 19; (g) J. Randrup and C.M. Ko, Nucl. Phys. A **343** (1980) 519; (h) J. Randrup, Phys. Lett. B **99** (1981) 9; (i) W. Zivermann, B. Schürmann, K. Dietrich and E. Martschew, Phys. Lett. B **134** (1984) 397; (j) W. Zwermann and B. Schürmann, Nucl. Phys. A **423** (1984) 525; (k) J. Cugnon and R.M. Lombard, Phys. Lett. B **134** (1984) 392; Nucl. Phys. A **422** (1984) 635; (l) H.W. Barz and H. Iwe, Phys. Lett. B **143** (1984) 55; (m) T.S. Biro, B. Lukacs, J. Zimanyi and H.W. Barz, Nucl. Phys. A **386** (1982) 617; Z. Phys. A **311** (1983) 311; (n) K.H. Müller, Nucl. Phys. A **395** (1983) 509; (o) C.M. Ko, Phys. Lett. B **120** (1983) 294; Phys. Lett. B **138** (1984) 361

Note added in proof: The work reported here has been continued in the course of the last nine months, with many of the presented estimates now being results of sophisticated dynamical calculations. See: P. Koch, B. Müller and J. Rafelski, Strangeness in Relativistic Heavy Ion Collisions, Phys. Rep. (1986) (in press), Preprint UCT-TP 41/86. J. Rafelski, Cape Town, 15 May 1986.